

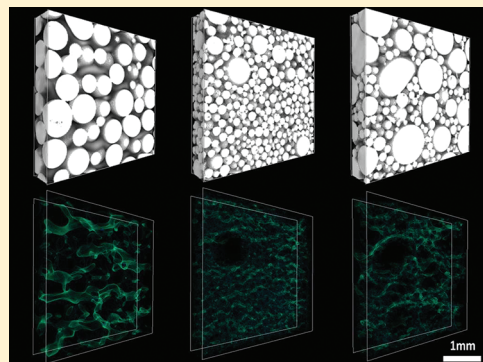
# Applicability of Colloid Filtration Theory in Size-Distributed, Reduced Porosity, Granular Media in the Absence of Energy Barriers

Eddy F. Pazmino,<sup>†</sup> Huilian Ma,<sup>†</sup> and William P. Johnson<sup>\*,†</sup>

<sup>†</sup>Department of Geology and Geophysics, University of Utah, Salt Lake City, Utah 84112, United States

**S** Supporting Information

**ABSTRACT:** The vast majority of colloid transport experiments use granular porous media with narrow size distribution to facilitate comparison with colloid filtration theory, which represents porous media with a single collector size. In this work we examine retention of colloids ranging in size from 0.21 to 9.1  $\mu\text{m}$  in diameter, in columns packed with uniform and size-distributed borosilicate glass bead porous media with porosity ranging from 0.38 to 0.28. Conditions were favorable to attachment (absent a significant energy barrier). The goal was to determine the applicability of colloid filtration theory to colloid retention in these media. We also directly observed deposition at the pore scale in packed flow cells. The pore domain was characterized via high resolution computerized X-ray micro tomography (HRXMT). The flow field was examined using Lattice-Boltzmann flow simulation methods (LBM). The influence of preferential flow paths on colloid retention in the lowest porosity media was accounted for by correcting the fluid velocity. Straining in pore throats too small to pass was not a significant contributor to colloid retention despite colloid-to-collector size ratios up to 0.05. Mechanistic simulations via the Ma-Pedel-Fife-Johnson correlation equation (MPFJ) for colloid filtration predicted the experimentally observed trends in deposition with porosity when a number-based mean grain size was used.



## INTRODUCTION

Over the past several decades scores of experiments have been performed to examine colloid filtration in granular porous media. Surprisingly, all of these experiments fall within the porosity range between 0.33 to 0.38. Notably, previous studies examining a wider range of porosities and porous media packing structures have been conducted under unfavorable conditions or under conditions where the regime (favorable versus unfavorable) was not established. Significantly decreased porosity requires not only a wide grain size distribution but also one characterized by particle size extremes, e.g. bimodal, or a carefully ordered packing structure. Many engineered and especially natural, granular media are distributed with respect to grain size. However, existing colloid filtration theory idealizes porous media using a single grain (collector) size. Hence, prediction of colloid transport via existing theory in size-distributed porous media requires determining the collector size that represents a given medium. The objective of this work was to extend classical filtration theory, which previously has been tested only in a narrow range of porosities.

To date, two studies have examined this issue: Martin et al.<sup>1</sup> and Porubcan and Xu,<sup>2</sup> who concluded that the volume-based  $d_{10}$  and number-based mean, respectively, best represented their distributed porous media for the purpose of predicting colloid retention. The two studies employed two different strategies. The strategy used by Martin et al.<sup>1</sup> was to identify the representative grain size that collapsed deposition efficiency versus

collision number onto a single trend, where collision number equals  $k_f \rho L$ ,  $k_f$  is the deposition rate coefficient,  $v$  is the average pore water velocity, and  $L$  is the column length. This strategy assumed that deposition efficiency should be independent of the different fluid velocity fields expected for the different porous media size distributions examined. However, subsequent research shows that deposition efficiency varies with fluid velocity,<sup>3</sup> indicating that the strategy may be compromised. Additionally, Martin et al.<sup>1</sup> examined only a single colloid size, limiting the generality of their observations. Although Martin et al.<sup>1</sup> examined both unfavorable and favorable conditions; they used a relatively high concentration of divalent salt to produce the latter condition, which risks reducing colloid–colloid repulsion to the point of driving colloid aggregation. The resulting deposition efficiencies were greater than unity, suggesting colloid aggregation did occur during those particular experiments.

Porubcan and Xu<sup>2</sup> examined multiple colloid sizes (0.46, 2.9, 5.1, 6.1  $\mu\text{m}$ ) under unfavorable deposition conditions. Their strategy was to identify the representative grain size that collapsed  $k_f$  versus ratio of particle to grain diameter ( $d_p/d_g$ ) onto a single trend under the assumption that straining was the mechanism of deposition. However, this assumption neglects the

**Received:** June 28, 2011

**Accepted:** October 26, 2011

**Revised:** October 22, 2011

**Table 1. Characteristic Grain Sizes for the Three Porous Media Studied**

porous medium	porosity	grain size ( $\mu\text{m}$ )					
		weight-based <sup>a</sup>			number-based <sup>a</sup>		
		$d_a$	$d_{gm}$	$d_{10}$	$d_a$	$d_{gm}$	$d_{10}$
uniform	0.38	510	510	-	510	510	-
monomodal nonuniform	0.34	414	372	222	225	210	183
bimodal nonuniform	0.28	507	425	214	169	147	115

<sup>a</sup>  $d_a$  and  $d_{gm}$  correspond to the arithmetic and geometric means;  $d_{10}$  corresponds to the size below which 10% of the overall collector population is smaller; weight and volume based  $d_{10}$  are equivalent because the density is the same for all collector size fractions.

possibility that deposition occurred in response to surface roughness or heterogeneity. Furthermore, a directly observed lack of straining in pore throats too small to pass in our experiments (described below) (maximum  $d_p/d_g$  ratio = 0.05) suggests that straining may not be the prevalent mechanism in the experiments of Porubcan and Xu<sup>2</sup> (maximum  $d_p/d_g$  ratio = 0.03). Although their experiments were conducted in quartz sands, where angularity of the media may create a different pore throat size distribution relative to glass beads of equivalent sieve size, it is important to note that surface roughness and charge heterogeneity could play an important role in colloid retention e.g., Johnson et al.<sup>4</sup> Porubcan and Xu<sup>2</sup> attributed the retention to straining on the basis that the trend for  $k_f$  as a function of colloid size was inconsistent with filtration theory. Specifically, lesser (negligible) deposition was observed for the 0.46  $\mu\text{m}$  colloid relative to the 2.9  $\mu\text{m}$  colloid. We would note, however, that the influent concentration was 3 orders of magnitude greater for the 0.46  $\mu\text{m}$  colloid relative to the 2.9  $\mu\text{m}$  colloid, possibly yielding large differences in ability to detect deposition.

Consistent with the existing literature, Martin et al.<sup>1</sup> and Porubcan and Xu<sup>2</sup> examined a narrow porosity range (0.32–0.38). The lack of experimental results over a larger porosity range stands in contrast with existing filtration theory, which explicitly includes porosity as a parameter that describes the flow field that delivers colloids to the collector surfaces.<sup>5</sup> Practically speaking, filtration theory has never been compared to experimental results conducted in granular media over a significant porosity range.

In this paper we conduct colloid filtration experiments in porous media spanning a larger porosity range than previously examined (0.28–0.38). The primary goal is to discern the influence of porosity on colloid retention in granular media and determine whether it is captured by colloid filtration theory. A necessary secondary goal is therefore to determine a representative collector size that reconciles experimental results to theoretical predictions. Since mechanistic theory is presently available only for favorable deposition conditions (absent of a colloid-surface energy barrier), the experiments were conducted under these conditions. Additional issues that arise under conditions of decreased porosity are the development of preferential flow paths and straining of colloids in pore throats too small to pass. We show that colloid deposition in the reduced porosity granular media was strongly influenced by preferential flow paths. We also observed that straining in pore throats too small to pass was not a significant influence on colloid deposition in the reduced porosity media under favorable conditions, suggesting that it may not be a major influence under unfavorable conditions.

## MATERIALS AND METHODS

**Materials.** Spherical monodispersed fluorescent carboxylate-modified polystyrene latex microspheres ranging in size from 0.21 to 9.1  $\mu\text{m}$  were used in the experiments. Injection concentration varied among the different sizes due to different light intensities among the different microsphere stocks, i.e. 1E6, 1E6, 1E6, 5E5, 1E5/mL for the 0.21, 1.1, 2.0, 4.4, 9.1  $\mu\text{m}$  sizes, respectively.

Borosilicate glass beads were sieved to produce discrete size fractions ranging from 850 to 74  $\mu\text{m}$ . The size fractions were combined to produce three porous media of different porosities (Table 1), including the following: 1) A uniform monodisperse porous medium (porosity 0.38), consisting solely of 510- $\mu\text{m}$  beads; 2) A bimodal nonuniform porous medium (porosity 0.28), consisting of predominant weight fractions of 850–600  $\mu\text{m}$  and 250–147  $\mu\text{m}$  beads; and 3) A monomodal (normally distributed by weight) nonuniform porous medium (porosity 0.34), consisting of beads ranging from 800 to 74  $\mu\text{m}$ . Detailed information of the porous media sources and size distributions are provided in the Supporting Information.

The glass beads and the flow cell used in direct observations were cleaned using the SC-1 cleaning procedure as described in Johnson et al.<sup>4</sup> A portion of the glass beads was coated with iron oxide according to Johnson and Logan.<sup>6</sup>

**Column Experiments.** All experiments were conducted under favorable attachment conditions using two strategies: 1) Using the cleaned glass beads and setting the solution ionic strength to 50 mM and pH to 2.0;<sup>7</sup> 2) Using iron oxide-coated glass beads and setting the solution ionic strength to 10 mM and pH to 6.72. Favorable conditions were replicated by using both strategies in the bimodal nonuniform medium for experiments involving 2.0 and 9.1  $\mu\text{m}$  colloids. Deposition was equivalent for both strategies; hence, these strategies are not distinguished in the results below. Log–linearity of colloid retention profiles (Supporting Information) was verified for all the experiments, reflecting favorable conditions for attachment. Solution pH was maintained using 2.2 mM MOPS buffer (3-(N-morpholino)propanesulfonic acid, 4-morpholinepropanesulfonic acid; Sigma–Aldrich Corp.) in all experiments. pH was controlled by preconditioning the columns extensively and measuring effluent pH at end of each experiment, showing small variation (<0.15 pH points) relative with the injected solution.

Cylindrical Plexiglas columns (20 cm long, 3.81 cm i.d.) were dry-packed with glass beads flushed with CO<sub>2</sub> and equilibrated with microsphere-free solution. The procedure of packing and pre-equilibration is described in previous publications.<sup>7,8</sup> After pre-equilibration, a solution with microspheres was injected, followed by elution using microsphere-free solution, and finally dissection of the porous media to recover retained colloids. The suspensions and solutions were injected in up-flow mode and in down-flow mode for selected experiments, using a syringe pump (Harvard Apparatus, Inc., Holliston, MA). During injection, aggregation and settling of microspheres were minimized by sonicating for 1 min and vertically rotating the syringe pump, every 15 min. Pore water velocities of 4.0 m/day, 3.3 m/day, and 3.0 m/day were examined in the bimodal nonuniform, monomodal nonuniform, and uniform media, respectively. Recovery of colloids from the sediment was conducted using well-established techniques.<sup>8</sup> Colloid concentrations in column effluent and recovered from sediment were determined via flow cytometry, as described in detail in the Supporting Information. Microscopic

observations of colloid suspensions conducted during the flow cell experiments consistently showed negligible colloid aggregation, as did flow cytometry analyses, where >95% of total counts corresponded to single particles.

**Flow Cell Experiments.** Direct observation of colloid retention was performed in a  $1 \text{ cm}^2 \times 4 \text{ cm}$  length flow-through quartz cell (46-Q-10, Starna Cells, Inc., Atascadero, CA) oriented horizontally over an inverted fluorescence microscope. The flow cell was evenly packed with the same porous media used in the column scale experiments. The microsphere suspension was introduced by a syringe pump (Harvard Apparatus, Holliston, MA), with an average pore water velocity a factor of 10 greater than the pore water velocity of the column experiments. This was done for each porous medium to prevent settling due to the low pumping rate required for this small volume cell. The cell was preconditioned for 60 min (pH = 2.0, IS = 50 mM NaCl) with microsphere-free solution. Details of the epifluorescence microscopy and image acquisition are provided in the Supporting Information. Observations were conducted by scanning across the entire surface of the flow cell from injection to outlet at different focal lengths and for several times during the experiment, to obtain representative information on the mechanisms of attachment at the flow cell scale.

**Data Analysis.** The overall recovery (mass balance) of colloids was determined by summing the numbers of retained colloids and colloids that exited the column. The total number of retained colloids was obtained by summing the colloids recovered from all column segments. The total number of colloids that exited the column was obtained by integrating the area under the breakthrough-elution curve. The colloid deposition rate coefficient was determined from the experimental effluent breakthrough and the profile of retained colloids using eqs 1 and 2, respectively

$$\ln \frac{C}{C_0} = -\frac{k_f}{v}x \quad (1)$$

where  $C$  is the microsphere concentration in the aqueous phase,  $C_0$  is the concentration of microspheres at the source,  $x$  is the travel distance in the column, and  $\theta$  is the porosity

$$S = \frac{\theta}{\rho_b} t_0 C_0 k_f e^{-\left(\frac{k_f}{v}x\right)} \quad (2)$$

where  $S$  is the concentration of microspheres in the sediment phase,  $\rho_b$  is the bulk density of the porous medium, and  $t_0$  is the duration of injection. The use of eqs 1 and 2 is justified by the fact that during steady state breakthrough, the transient portion of the breakthrough curve has given way to a steady state plateau, and so the concentrations are no longer significantly influenced by dispersion relative to retention. Both the effluent breakthrough-elution curve and the retained profiles were fit when they were available. In all cases the retained profile was available. However, in some experiments no breakthrough occurred.

Tracer breakthrough curves were simulated using the two region model in CXTFIT,<sup>9,10</sup> according to the following equation

$$\theta_m \frac{\partial c_m}{\partial t} = \theta_m D_m \frac{\partial^2 c_m}{\partial x^2} - \theta_m v_m \frac{\partial c_m}{\partial x} - \alpha(C_m - C_{im}) \quad (3)$$

$$\theta_{im} \frac{\partial c_{im}}{\partial t} = \alpha(C_m - C_{im}) \quad (4)$$

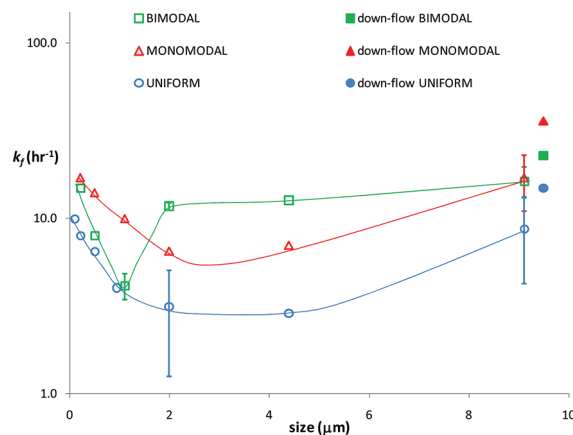


**Figure 1.** Experimental  $k_f$  values for the three different porous media studied: 1) uniform ( $\theta = 0.38$ ); 2) monomodal nonuniform ( $\theta = 0.34$ ); and 3) bimodal nonuniform ( $\theta = 0.28$ ). The open symbols correspond to column experiments conducted in down-flow and closed symbols experiments conducted in up-flow mode. Data for uniform media and colloids  $< 2 \mu\text{m}$  correspond to Tong and Johnson<sup>7</sup> and Li et al.<sup>8</sup> Trend lines connect data points for ease of presentation. Error bars denote maximum and minimum values.

where  $\theta_m$  is the mobile porosity,  $\theta_{im}$  is the immobile porosity,  $C_m$  is the aqueous concentration in the mobile region, and  $C_{im}$  is the aqueous concentration in the immobile region.  $D_m$  is the hydrodynamic dispersion coefficient in the mobile region,  $v_m$  is the average pore water velocity in the mobile pore space, and  $\alpha$  is a first order coefficient describing colloid transfer from mobile to immobile regions.

Three dimensional reconstructions of each porous media were obtained using HRXMT described in Miller and Lin<sup>11</sup> and in the Supporting Information. A cubic subset (2.8 mm sides,  $5.02 \mu\text{m}$  resolution) of the HRXMT reconstruction was used to solve the fluid flow field using Lattice Boltzmann methods (LBM).<sup>12</sup> Pore size distribution was obtained using the same procedure described in Li et al.<sup>13</sup> and in the Supporting Information.

## RESULTS

With respect to colloid retention as a function of colloid size, all three media (both uniform and nonuniform) demonstrated the expected minimum value of  $k_f$  corresponding to colloid sizes in the one to several  $\mu\text{m}$  size range (Figure 1). The small variation in pore water velocity (3.0–4.0 m/day) is expected to yield small variation in  $k_f$  values (<8%) according to CFT, and this change is <3% of the range of  $k_f$  values across the colloid size range. The trends with colloid size for the three media indicate that  $k_f$  generally increased with decreasing porosity (in qualitative agreement with classic filtration theory as discussed below). However, the trends differed for the bimodal medium relative to the monomodal and uniform media in two important respects:

- 1) Disproportionately low values were observed for the bimodal nonuniform media for the  $< 2.0 \mu\text{m}$  colloid size range
- 2)  $k_f$  values were approximately the same among the two nonuniform media for the  $9.1 \mu\text{m}$  colloid size. These exceptions will be discussed further below.

The values of  $k_f$  observed in the uniform media showed reasonable agreement with predicted values from the LH, MPFJ, TE, and NG correlation equations;<sup>14–18</sup> i.e., experimental data

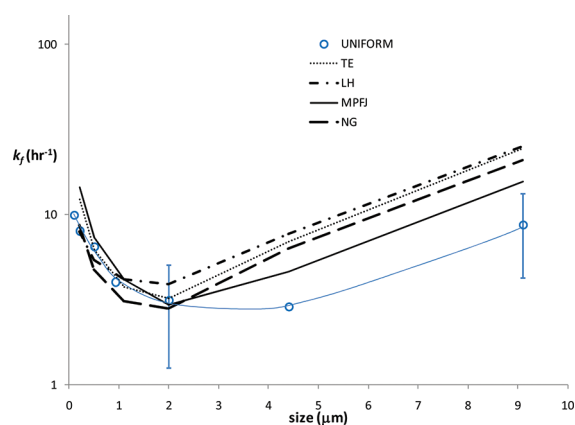


**Figure 2.** Experimental  $k_f$  results (open circles) for uniform porous media, collector size  $510 \mu\text{m}$ , and predictions from four correlations: LH,<sup>14</sup> MPFJ,<sup>15,16</sup> TE,<sup>17</sup> and NG.<sup>18</sup> Error bars denote maximum and minimum values.

and predictions agreed within a factor of 2–3 for all colloid sizes (Figure 2), reflecting favorable conditions of attachment in the experiments. Predictions from the original Happel-based model (RT model)<sup>5</sup> are not shown due to their similarity to the TE model predictions. For colloid sizes of  $2 \mu\text{m}$  and larger, the predicted values of  $k_f$  using the TE, LH, NG and to a lesser extent MPFJ, correlation equations are higher and show a steeper slope relative to the experimental results. The lower  $k_f$  values predicted for the larger colloids by the MPFJ model (relative to the other models) result from the grain-to-grain contact influence on the flow field, as described in Ma et al.<sup>19</sup>

The experiments were largely run in up-flow mode, where the flow direction was opposite to gravity, as typically performed in order to minimize air trapping during saturation and equilibration of the columns. In contrast, the mechanistic models underlying the correlation equations are based on force balance simulations involving down-flow mode. The effect of gravity may be significant for microspheres larger than approximately  $2 \mu\text{m}$ ; hence, additional experiments were run in down-flow mode for the  $9.1\text{-}\mu\text{m}$  microspheres (Figure 1). Values of  $k_f$  were increased in down-flow mode relative to up-flow mode by a factor of 2 or less, which is similar to the error of the experiment but which likely reflects the effect of gravity, since this effect was observed for all three porous media (Figure 1). The down-flow results for the monomodal nonuniform medium more closely match theory (Figure 2), as expected since the underlying numerical models were run in down-flow mode.<sup>14–18</sup> A detailed analysis of the effect of orientation of flow relative to gravity on colloid retention under favorable conditions can be found in Ma et al.<sup>20</sup>

The average mass recovery (Supporting Information) from all experiments was 87%, reflecting good experimental recovery. In the few individual cases where recovery was low, the general trend of the retention profile was used to guide a model fit that accounted for all injected colloids. All experimental retention profiles were log linear, corroborating favorable conditions of attachment.

## DISCUSSION

The relatively low values of  $k_f$  for  $<2 \mu\text{m}$  and the  $9.1 \mu\text{m}$  size colloids observed for the bimodal medium likely reflect

influences of the porous media structure not accounted for in colloid filtration theory. HXRMT images of the three porous media reveal increasingly nonuniform structure in the order from uniform, monomodal nonuniform, and bimodal nonuniform media (Supporting Information).

Breakthrough curves from tracer tests (Figure 3 top) show increasing dispersion in the order from uniform, monomodal nonuniform, and bimodal nonuniform media.

The two-region model fits (CXTFIT) indicate that practically all pore space was mobile for the uniform and monomodal nonuniform media, as shown by unitary ratios of mobile to total porosity backed out from the simulations (Figure 3 top). In contrast, the model fits to the bimodal medium indicated that a fraction of the pore space was immobile. The fraction of mobile pore space relative to total pore space ( $\theta_m/\theta$ ), for which a good fit to the tracer breakthrough was obtained, ranged from 10% to 60%, with the mass rate transfer coefficient ( $\alpha$ ) correspondingly ranging from 12 to  $2.33 \text{ h}^{-1}$ . The hydrodynamic dispersion coefficient of the mobile phase  $D_m$  fitted from the uniform and monomodal nonuniform media tracer tests was  $0.012 \text{ cm}^2 \text{ min}^{-1}$ . The values of  $\theta_m/\theta$  and  $\alpha$  backed out from nonlinear least-squares analyses were 48% and  $4 \text{ h}^{-1}$ , respectively. For a given discharge, the pore water velocity in mobile pore space must increase proportionally to the fraction of immobile pore space. Because the deposition rate coefficient varies with fluid velocity, the relatively low values of  $k_f$  observed for the  $<2.0$  and  $9.1 \mu\text{m}$  colloids in the bimodal nonuniform medium (Figure 2) may reflect the effect of higher fluid velocity in the preferential flow paths in this medium, as discussed further below.

CXTFIT allows a simple approximate characterization of preferential flow paths in terms of mobile and immobile pore space in the bimodal nonuniform media. In reality a distribution of fluid velocities exists in the porous media, which were explored using Lattice-Boltzmann simulations in the HRXMT-rendered pore domains. The resulting pore water velocity distributions in each porous media are shown for the three media (Figure 3 bottom). The LB flow field for the uniform porous medium shows relatively large advective pore domains evenly distributed through the medium. In contrast, the LB flow field for the monomodal nonuniform porous medium shows relatively small advective pore domains that are also evenly distributed through the medium. In further contrast, the LB flow field for the bimodal nonuniform media shows relatively small advective pore domains that are not evenly distributed through the media, indicating a larger contrast between mobile and immobile pore space in the bimodal medium relative to the other two media.

Volume-averaged permeabilities derived from the LB flow fields were  $0.19 \times 10^{-6}$  and  $0.21 \times 10^{-6} \text{ cm}^2$  for the bimodal and monomodal nonuniform media (corresponding to very fine sand or silt), respectively, which is a factor of 5 lower than the uniform media ( $1.10 \times 10^{-6} \text{ cm}^2$ ). Although the two nonuniform media show similar permeabilities, the bimodal medium is distinguished by its uneven spatial distribution of advective pore domains.

The combined XMT, Lattice-Boltzmann, and tracer test results indicate that only a fraction of the pore domain in the bimodal nonuniform media was significantly advective. The value of 48% mobile porosity backed out from nonlinear least-squares optimization was herein used to represent the fraction of advective pore domain in the bimodal medium in order to demonstrate the effect of the preferential flow paths in colloid transport, yielding an average pore water velocity in the advective pore space of the medium two times greater than the

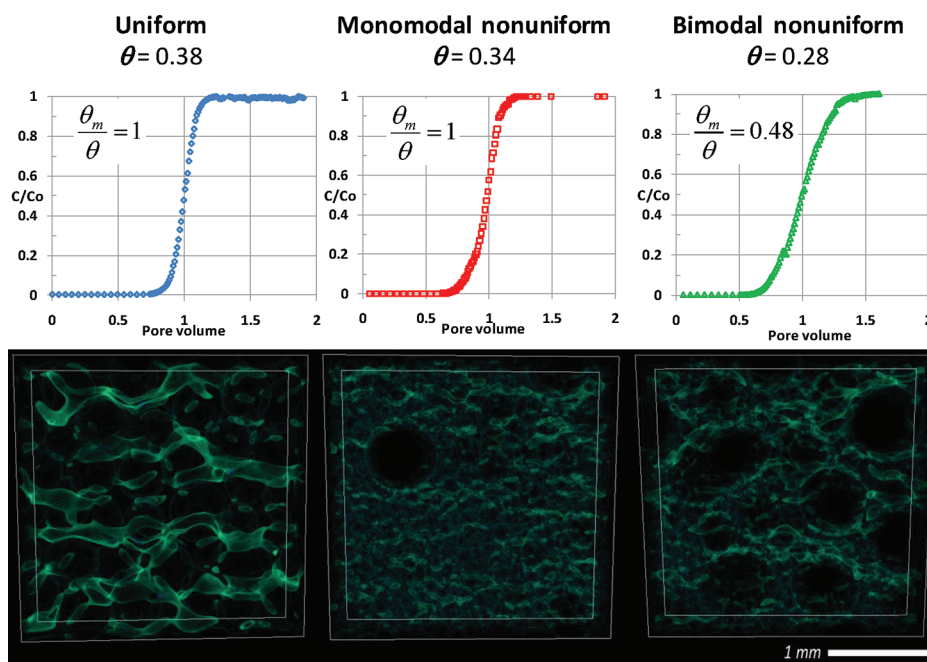


**Figure 3.** Top: tracer breakthrough curves for each media and ratios of mobile to total porosity shown. Bottom: corresponding flow field of each porous media obtained from LBM. Fluid velocities in the lower 30% of the velocity histogram distribution are shown in blue; fluid velocities in the upper 30% are shown in green.

whole-domain-averaged pore water velocity. Since the bulk of colloid flux was carried in the advective pore domain, a simple correction for the corresponding fluid velocity can be performed to yield an approximate corrected value for  $k_f$  from eqs 1 and 2. The resulting trends in  $k_f$  as a function of colloid size are shown in Figure 4, where it is seen that, with the velocity correction for the bimodal media,  $k_f$  increases with decreasing porosity across the entire porosity range examined. It should be noted that the velocity correction was equivalent for all colloid sizes for lack of a known method to account for possible differential effects of preferential flow paths among the colloid sizes (due to differing diffusion coefficients). This potential differential effect may contribute to different trend in  $k_f$  versus colloid size for the bimodal relative to the other media.

The preponderance of the 147–250  $\mu\text{m}$  collector size fraction in the bimodal medium yields ratios of particle to grain diameter ( $d_p/d_g$ ) in the range of 0.05 for the 9.1  $\mu\text{m}$  microspheres. Given that previous studies infer straining to be the mechanism of deposition under much lower  $d_p/d_g$  ratios, e.g. 0.008, 0.003,<sup>2,21</sup> the potential role of straining in our results warrants further examination. The pore size distributions obtained for the three porous media from HRXMT images (Supporting Information) show that only a very small fraction of pore throats existed in the <10  $\mu\text{m}$  size range, i.e., 0.08, 0.08, and 0.66% for the uniform, monomodal nonuniform, and bimodal non uniform media, respectively. These small fractions of the pore space may potentially trap 9.1- $\mu\text{m}$  colloids. For example, given that nearly 1% of the HRXMT-rendered domains had <10- $\mu\text{m}$  pores (nonuniform media), we can reasonably estimate that 0.1% of injected colloids would be retained via straining in pore throats too small to pass, allowing 99.9% of injected colloids to move through the 2.8-mm HRXMT domain. Approximately 70 such domains would exist along a 20-cm column, yielding a probability of exiting the column equal to  $0.999^{70}$  or 93%, which corresponds

to 7% of colloids being retained. However, in contrast to this probabilistic estimate, direct observations showed no evidence of straining in pore throats, which were much larger than even the largest colloid size observed. Attachment occurred predominantly on the upstream open surface of the glass beads. Regardless of the higher fluid velocity of the flow cell relative to the column, any physical straining should manifest in both experiments because physical straining occurs independent of fluid velocity. There was no evidence of physical straining in pore throats, which were much larger than even the largest colloid size observed, and this is documented in images and movies in the Supporting Information.

The clear inverse relationship between porosity and  $k_f$  observed in Figure 4 appears to not be driven by straining and is therefore expected to reflect the influence of mass transfer processes that are enveloped in classic filtration theory. The trends in  $k_f$  as a function of colloid size obtained under favorable deposition conditions provide a platform for comparison to mechanistic theoretical predictions (Figure 4). The theoretical unit cell predictions are based on a representative collector size, for which there are multiple options to choose from, including arithmetic versus geometric means as well as number-based versus weight-based size fractions. The number-based mean grain size (based on numbers of collectors within each size fraction) is lower than the weight-based mean grain size (based on the weight of collectors within each size fraction) (Table 1). The number-based arithmetic means are 169 and 224  $\mu\text{m}$  for the bimodal and monomodal media, respectively, whereas the weight-based arithmetic means are 507 and 414  $\mu\text{m}$  for the bimodal and monomodal media, respectively. Figure 4 shows that the weight-based mean grain size does not reflect the sensitivity to porosity that was observed in the experiments (Figure 4a), and this is also true if one develops a composite  $k_f$  by determining  $k_f$  for each size fraction and then averaging according

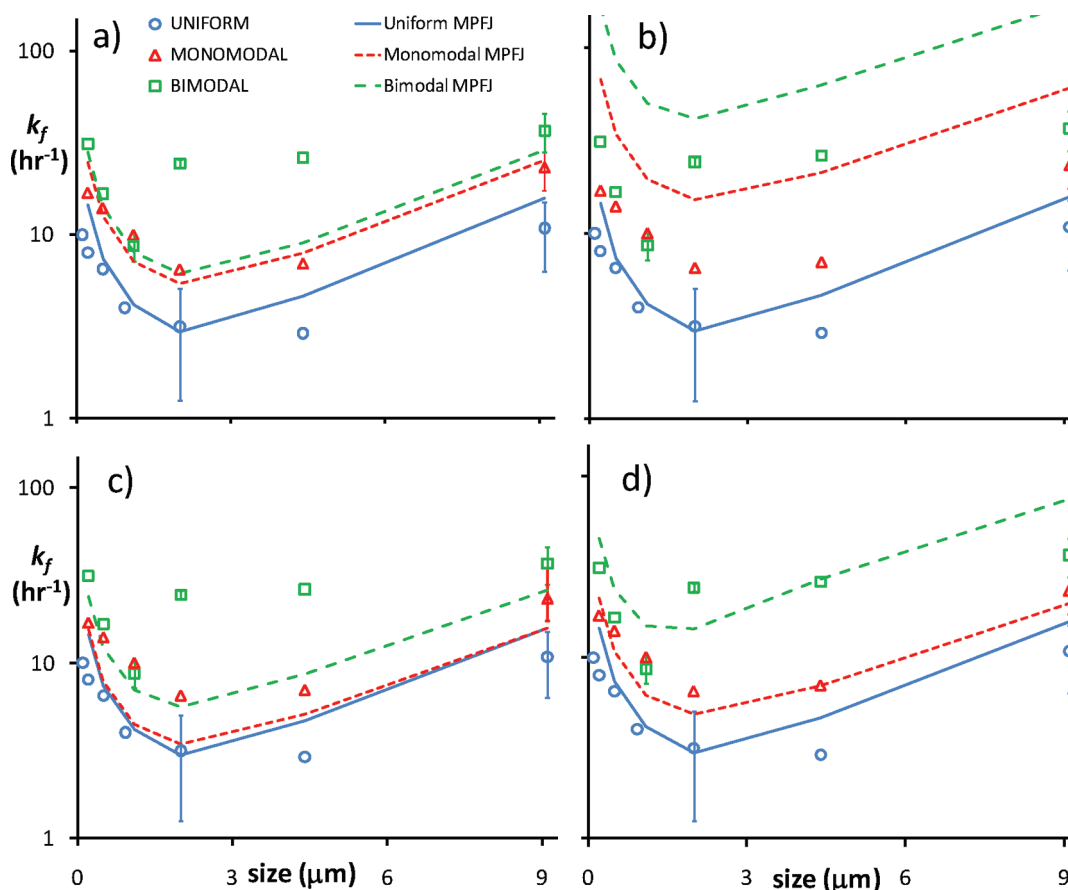


**Figure 4.** Comparison between experimental data (open symbols) of uniform (blue), monomodal nonuniform (red), and bimodal nonuniform (green) porous media with  $k_f$  predictions using the MPFJ correlation (lines) for different collector sizes: (a) weight based mean, (b) number based mean, (c) composite weight-based  $k_f$ , and (d) composite number-based  $k_f$ . Corrected experimental  $k_f$  values for the bimodal nonuniform medium are shown after the effect of preferential flow paths is considered. Error bars denote maximum and minimum values.

to the weight-based contribution to the total size distribution (Figure 4c). In contrast, the number-based mean grain size does capture the experimentally observed sensitivity of  $k_f$  to porosity (Figure 4b), although the absolute values of  $k_f$  predicted by the number-based mean grain size are higher than the experimental values (Figure 4b). Notably, this overprediction is largely eliminated by use of a composite number-based  $k_f$  (Figure 4d). The corresponding sums of squares of log residuals were 0.66, 3.36, 1.03, and 0.33 for the weight-based arithmetic mean, number-based arithmetic mean, composite weight-based  $k_f$ , and composite number-based  $k_f$ , respectively (Supporting Information). The number-based geometric mean and the weight-based  $d_{10}$ , are similar to the number-based arithmetic mean (Table 1). Therefore, predictions using the number-based geometric mean and weight-based  $d_{10}$  would yield similar values as the ones shown in Figure 4b.

By comparing experimental observations and theoretical predictions for deposition in grain size-distributed media, we herein provide a theory-based approach for determining the appropriate grain size with which to represent a porous medium for prediction of colloid deposition. Our finding, that the number-based mean captures the sensitivity of  $k_f$  to porosity, is consistent with the conclusions of Martin et al.<sup>1</sup> and Porubcan and Xu<sup>2</sup> who concluded that the volume-based  $d_{10}$  and number-based mean, respectively, best represented their distributed porous media.

Both of these parameters emphasize the smaller size fractions of the porous media size distribution. However, improved predictions were obtained by determining  $k_f$  for each size fraction and then averaging according to the number-based contribution to the total distribution (Figure 4d). This indicates that a single representative grain size did not fully reflect the mass transfer processes for the overall porous media grain size distribution, reflecting a limitation of the unit cell approach, which idealizes the porous media using a single grain or pore-scale representative structure. The observed influence of preferential flow paths on colloid deposition also highlights a limitation of single-pore unit cells, since they cannot explicitly capture this attribute of porous media.

Although assemblage-scale (e.g., Figure 3 bottom) mechanistic simulations of colloid transport have been performed under favorable deposition conditions e.g. Long and Hilpert,<sup>15</sup> it is doubtful that accurate colloid transport simulations at this scale are numerically tractable for unfavorable deposition conditions, suggesting the need for a hybrid approach that combines the tractability of the unit cell approach with the representativeness of the fluid flow field at the assemblage scale.

One of the most important findings of extending colloid filtration experiments to lower porosities is the determination that the observed values of  $k_f$ , and their trends with colloid size, are described by classic filtration theory. This finding, and the

direct observation that no straining was evident in pore throats too small to pass even for  $d_p/d_g$  ratios up to 0.05, suggest that the  $d_p/d_g$  threshold of 0.003–0.008, below which physical straining is inferred to predominate,<sup>2,21</sup> is not a general threshold. These threshold values were reported from experiments conducted in quartz sand media,<sup>2,21</sup> where angularity of the quartz sand grains may affect the pore throat size distribution. However, no direct evidence (e.g., microscopic observations) was provided to determine the prevalence of physical straining relative to retention on the open surface via surface charge heterogeneity and surface roughness. Furthermore, in experiments comparing transport in quartz sand, no entrapment in pore throats too small to pass was observed, despite the colloid-collector size ratio being 0.046 even for the average grain size in the distribution.<sup>13</sup> Both observation and theory clearly showed that the colloid deposition observed in our experiments was physicochemical in nature. Even if such deposition would eventually lead to colloid aggregation in, and eventual clogging of, pore throats, it should be addressed mechanistically via physicochemical processes such as colloid–colloid interaction and accumulation and is not mechanistically represented by straining in pore throats too small to pass.

## ■ ASSOCIATED CONTENT

**S Supporting Information.** Additional information is provided. Tables S1–S3, Figures S1–S4, and a Time-lapse Series S1. This material is available free of charge via the Internet at <http://pubs.acs.org>.

## ■ AUTHOR INFORMATION

### Corresponding Author

\*Phone: (801) 664-8289. E-mail: [william.johnson@utah.edu](mailto:william.johnson@utah.edu).

## ■ ACKNOWLEDGMENT

This article is based upon work supported by the National Science Foundation Chemical, Biological, and Environmental Transport, and Hydrologic Science Programs (0822102). Any opinions, findings, and conclusions or recommendations expressed in this material are those of the authors and do not necessarily reflect the views of the National Science Foundation. We thank Professors Jan Miller and C. L. Lin at the Department of Metallurgical Engineering of the University of Utah for their assistance in generating XMT reconstructions of the porous media and LBM simulation of fluid flow fields. Finally we would like to thank the four anonymous reviewers for their helpful comments.

## ■ REFERENCES

- (1) Martin, M. J.; Logan, B. E.; Johnson, W. P.; Jewett, D. G.; Arnold, R. G. Scaling bacterial filtration rates in different sized porous media. *J. Environ. Eng.* **1996**, *122* (5), 407–415.
- (2) Porubcan, A. A.; Xu, S. Colloid straining within saturated heterogeneous porous media. *Water Res.* **2011**, *45* (4), 1796–1806.
- (3) Li, X.; Zhang, P.; Lin, C. L.; Johnson, W. P. Role of hydrodynamic drag on microsphere deposition and re-entrainment in porous media under unfavorable conditions. *Environ. Sci. Technol.* **2005**, *39* (11), 4012–4020.
- (4) Johnson, W. P.; Pazmino, E.; Ma, H. Direct observations of colloid retention in granular media in the presence of energy barriers, and implications for inferred mechanisms from indirect observations. *Water Res.* **2009**, *44* (4), 1158–1169.

- (5) Rajagopalan, R.; Tien, C. Trajectory analysis of deep-bed filtration with the sphere-in-cell porous media model. *AIChE J.* **1976**, *22* (3), 523–533.

- (6) Johnson, W. P.; Logan, B. E. Enhanced transport of bacteria in porous media by sediment-phase and aqueous-phase natural organic matter. *Water Res.* **1996**, *30* (4), 923–931.

- (7) Tong, M.; Johnson, W. P. Excess colloid retention in porous media as a function of colloid size, fluid velocity, and grain angularity. *Environ. Sci. Technol.* **2006**, *40* (24), 7725–7731.

- (8) Li, X.; Scheibe, T. D.; Johnson, W. P. Apparent decreases in colloid deposition rate coefficients with distance of transport under unfavorable deposition conditions: A general phenomenon. *Environ. Sci. Technol.* **2004**, *38* (21), 5616–5625.

- (9) van Genuchten, M. T.; Wagenet, R. J. Two-Site/Two-Region Models for Pesticide Transport and Degradation: Theoretical development and analytical solutions. *Soil Sci. Soc. Am. J.* **1989**, *53* (5), 1303–1310.

- (10) *The CXTFIT code for estimating transport parameters from laboratory or field tracer experiments*; U. S. Salinity Laboratory Agricultural Research Service; United States Department of Agriculture: Riverside, CA, 1999. [www.ars.usda.gov/services/software/92/cxftfit.pdf](http://www.ars.usda.gov/services/software/92/cxftfit.pdf) (accessed January 20, 2011).

- (11) Miller, J. Lin, C. L., High resolution X-ray micro CT (HRXMT) – Advances in 3D particle characterization for mineral processing operations. In *Recent Advances in Mineral Processing Plant Design*; Malhotra, D., Taylor, P., Spiller, E., LeVier, M., Eds.; Society of Mining, Metallurgy, and Exploration, Inc.: 2009; p 48.

- (12) Videla, A. R.; Lin, C. L.; Miller, J. D. Simulation of saturated fluid flow in packed particle beds--The lattice-Boltzmann method for the calculation of permeability from XMT images. *J. Chin. Inst. Chem. Eng.* **2008**, *39* (2), 117–128.

- (13) Li, X.; Lin, C. L.; Miller, J. D.; Johnson, W. P. Pore-scale observation of microsphere deposition at grain-to-grain contacts over assemblage-scale porous media domains using x-ray microtomography. *Environ. Sci. Technol.* **2006**, *40* (12), 3762–3768.

- (14) Long, W.; Hilpert, M. A correlation for the collector efficiency of Brownian particles in clean-bed filtration in sphere packings by a Lattice-Boltzmann method. *Environ. Sci. Technol.* **2009**, *43* (12), 4419–4424.

- (15) Ma, H.; Johnson, W. P. Colloid retention in porous media of various porosities: Predictions by the hemispheres-in-cell model. *Langmuir* **2010**, *26* (3), 1680–1687.

- (16) Ma, H.; Johnson, W. P. Erratum: Colloid retention in porous media of various porosities: Predictions by the hemispheres-in-cell model (Langmuir (2010) 26 (1680)). *Langmuir* **2010**, *26* (9), 6864.

- (17) Tufenkji, N.; Elimelech, M. Correlation equation for predicting single-collector efficiency in physicochemical filtration in saturated porous media. *Environ. Sci. Technol.* **2004**, *38* (2), 529–536.

- (18) Nelson, E.; Ginn, T.; New collector efficiency equation for colloid filtration in both natural and engineered flow conditions. *Water Resour. Res.* **2011**, *47*, W05543; DOI 10.1029/2010WR009587

- (19) Ma, H.; Pedel, J.; Fife, P.; Johnson, W. P. Hemispheres-in-cell geometry to predict colloid deposition in porous media. *Environ. Sci. Technol.* **2009**, *43* (22), 8573–8579.

- (20) Ma, H.; Pazmino, E.; Johnson, W. P. Gravitational settling effects on unit cell predictions of colloid retention in porous media in the absence of energy barriers. *Environ. Sci. Technol.* **2011**, *45* (19), 8306–8312.

- (21) Bradford, S. A.; Tadassa, Y. F.; Pachepsky, Y. Transport of giardia and manure suspensions in saturated porous media. *J. Environ. Qual.* **2006**, *35* (3), 749–757.